Journal of Applied Fluid Mechanics, Vol. 12, No. 2, pp. 603-615, 2019.
Available online at www.jafmonline.net, ISSN 1735-3645, EISSN 1735-3645.
DOI: 10.29252/jafm.12.02.28548

A Magnetohydrodynamic Time Dependent Model of Immiscible Newtonian and Micropolar Fluids through a Porous Channel: a Numerical Approach

M. Devakar† and Ankush Raje

Department of Mathematics, Visvesvaraya National Institute of Technology, Nagpur-440010, India.

†*Corresponding Author Email: m_devakar@yahoo.co.in*

(Received October 26, 2017; accepted August 20, 2018)

ABSTRACT

The objective of the present article is to study the magnetohydrodynamic(MHD) unsteady flow and heat transfer of two immiscible micropolar and Newtonian fluids through horizontal channel occupied with porous medium. Initially, fluids in both regions as well as both plates are at rest. At an instant of time, the flow in both regions is generated by a constant pressure gradient. The governing non-linear and coupled partial differential equations of Eringen's micropolar fluid and Newtonian fluid are solved subject to suitable initial, boundary and interface conditions. The numerical results for velocity, microrotation and temperature are obtained using Crank-Nicolson finite difference approach. The results obtained for velocities, microrotation and temperatures are presented through figures. The analysis regarding volume flow rate, skin-friction co-efficient and Nusselt number is also done and is presented through tables. It is explored that, velocity, microrotation and temperature are increasing with time and accomplishing steady state at higher time level. Velocity is decreasing with micropolarity parameter and Hartmann number, and increasing with Darcy number. Temperature enhances with increasing Brinkmann number, and declines with Prandtl number and ratio of thermal conductivities.

Keywords: Micropolar fluid; Immiscible fluid; Unsteady flow; MHD flow; Heat transfer; Porous medium.

NOMENCLATURE

Br	Brinkmann number
c	component of microrotation
C_f	skin friction co-efficient
C_p	specific heat ratio
C_{P1}, C_{P2}	specific heats of fluids
Da	Darcy number
F	interface
G	constant pressure gradient
h	spatial step size
$2h_1$	distance between plates
H_0	magnetic field strength
I	subscript of distinct fluid regions
J	gyration parameter
k^*	permeability of porous medium
k	temporal step size
K	thermal conductivity ratio
K_1, K_2	thermal conductivities of fluids
l	number of mesh points in spatial domain
m_1	viscosity ratio
M	Hartmann number
n_1	micropolarity parameter
Nu	Nusselt number
p	fluid pressure
Pr	Prandtl number
$\bar{q}$	fluid velocity vector
Q	volume flow rate
Re	Reynolds number
T_0^*	initial temperature of fluids
T_0	non-dimensional initial temperature of fluids
T_1, T_2	fluid temperatures
T_{w1}, T_{w2}	temperatures of plates
u_1, u_2	components of fluid velocities
U	maximum velocity in the channel
β	gyro-viscosity co-efficient
κ	vortex viscosity coefficient
μ_1, μ_2	viscosity co-efficients
$\bar{\upsilon}$	microrotation vector
ρ_1, ρ_2	density of fluids
σ	electrical conductivity of fluids

1 INTRODUCTION

Researchers across the globe have been in search of a convincing model over classical Newtonian fluid model to explain the behaviour of real fluids like lubricating oil, blood, etc. In early sixties, Eringen (1966) has proposed a non-Newtonian fluid model, called micropolar fluid model, to describe fluids of different shape, which may shrink and expand, may rotate independently of the rotation and movement of the fluid. Micropolar fluid belongs to a family of fluids, where the stress tensor is not symmetric. These fluids exhibit couple stresses, and the particles of the fluids have independent rotation called microrotation in addition to translational and angular velocities. The applications of micropolar fluid flows (Allen and Kline 1971) can be perceived in the design of thrust bearing, radial diffusers, transpiration drag reduction etc. The micropolar fluid posseses load carrying capacity better than the Newtonian fluid (2011). This fluid has also been used successfully to model the blood flow through blood vessels (Kang and Eringen 1976; Stokes 1971; Mekheimer and Kot 2008). Extensive work on the micropolar fluid theory and its applications have been documented in Ariman *et al*. (1973; 1974) and also in books written by Lukaszewicz (1999), Eringen (2000) and Stokes (1984). Due to its importance in engineering, numerous researchers showed attentiveness in the research on micropolar fluid flows. Cheng (2006) discussed the flow of micropolar fluid through vertical channel, where the fully developed flow was considered along with the free convective heat and mass transfer. Bataineh *et al*. (2009) explored homotopy analysis method and obtained the solution of free convective flow of micropolar fluid in a channel. In their work, Abdullaha and Amin (2010) discussed the blood flow through stenotic artery using micropolar fluid model. Recently, Mabood and Ibrahim (2016) studied the MHD convective flow over a stretching sheet in a micropolar fluid with radiation and Soret effects.

Worldwide, the study of magnetohydrodynamic flows is being carried out at an enormous rate due to its importance and applications in crucial fields such as magnetic drug targeting, aerospace engineering, astrophysics etc. Plenty of research work on magnetohydrodynamic flows can be seen in literature. Ashraf *et al*. (2013) studied the MHD micropolar fluid flow and heat transfer in channel. Prasad *et al*. (2013) discussed the power law fluid flow with thermal radiation and magnetohydrodynamic effects. Ramesh and Devakar (2015a) carried out a theoretical study on the magnetohydrodynamic peristaltic couple stress fluid flow in an inclined channel with heat transfer. The flow through porous medium is of foundational importance in chemical engineering, biomechanics etc. The presence of porous medium is noted in applications like movement of underground water and oils, filtration of fluids, functioning of human lung etc. In view of these distinguished applications, the research on flow through porous medium is carried out extensively in several contexts (See Naduvinamani and Santosh (2011), Bhargava *et al*. (2003) and the references therein).

The study of immiscible fluid flows is of practical importance in the petroleum extraction, crude oil transport, chemical industries, geophysics, plasma physics etc. Further, the evidences of these types of flows can be perceived in blood flow through arteries (Chaturani and Samy 1985). Bird *et al*. (1960) have given exact solutions of two immiscible Newtonian fluids. Later, Kapur and Shukla (1962) provided solutions of immiscible fluid flows between two parallel plates. Chamkha (2000) studied the flow of two viscous, incompressible, electrically conducting immiscible fluids in non-porous and porous channels under heat transfer effects. Singh (2005) has studied convective flow of two immiscible viscous fluids. Prathap Kumar *et al*. (2010) obtained the velocity and microrotation for natural-convective flow of micropolar and Newtonian fluids. Tetbirt *et al*.(2016) considered the micropolar and viscous fluids in vertical channel and numerically studied the velocity distribution, under magnetic effects. The fluid flow and heat transfer is widely used in functioning of thermoelectric cooler, thermal insulators, thermocouple etc. Further, this concept is prominently being used in heat exchanger which is widely used in refrigeration and air conditioning. The heat transfer aspect of immiscible fluid flows has been studied by various researchers in view of aforementioned applications. Zivojin *et al*.(2010) provided analytical solutions for a two-fluid flow between moving plates under MHD and heat transfer effects. Nikodijevic *et al*. (2011) discussed the MHD Couette flow for two-fluid case, in presence of heat transfer. Kumar and Gupta (2012) discussed the flow of immiscible micropolar and Newtonian fluids. They have considered natural convective flow with MHD effects. Ramana Murthy and Srinivas (2013) carried out thermodynamic analysis for immiscible micropolar fluid flows in a channel. Ramesh and Devakar (2015b) analysed the heat transfer characteristics for second grade fluid in a vertical channel.

The immiscible fluid flow problems that have been cited above are time independent. However, many practical problems concerning immiscible fluid flows are time dependent in nature. The unsteady immiscible fluid flows are more appropriate for understanding the applications in biomechanics, hydrology, crude oil transportation etc. In spite of its significance, because of the inherent complexities, the unsteady flows of immiscible fluids are not much explored. Nevertheless, some researchers studied the immiscible fluids flows in unsteady circumstances. Sai (1990) studied time dependent flow of two Newtonian fluids over a porous bed. The unsteady flow of immiscible conducting fluids between porous beds is discussed by Vajravelu *et al*. (1995). Further, the unsteady flows of immiscible Newtonian fluids with heat transfer are studied by Umavathi *et al*.(2005) and Umavathi *et al*. (2012). In current investigation, the unsteady magnetohydrodynamic flow of immiscible micropolar and Newtonian fluids through a channel occupied with porous medium is studied considering heat transfer effects. The governing non-linear coupled differential equations with initial, boundary and interface conditions are solved for flow variables using Crank-Nicolson

(1947) finite difference approach. Further, the volume flow rate, skin friction co-efficient and Nusselt number at channel walls, are carried out numerically.

2. MATHEMATICAL FORMULATION

Consider the unsteady and unidirectional flow of two immiscible, incompressible micropolar and Newtonian fluids through a horizontal channel. The horizontal channel comprises of fixed upper and lower plates separated by a distance $2h_1$ apart extending in x and z directions. The lower plate $y = -h_1$ is kept at constant temperature T_{w1} and the upper plate $y = h_1$ is kept at constant temperature T_{w2}. The channel is occupied with homogeneous porous medium of permeability k^*. Both fluids are assumed electrically conductive having electrical conductivity σ, and a constant transverse magnetic field of strength H_0 is applied to both the plates as shown in Fig. 1. As the fluids are assumed to be immiscible they constitute two fluid flow regions. The micropolar fluid is considered in lower region ($-h_1 \le y \le 0$), having density ρ_1, viscosity μ_1, vortex viscosity κ, thermal conductivity K_1, specific heat capacity C_{P1} and, the Newtonian fluid is considered in upper region ($0 < y \le h_1$), having density ρ_2, viscosity μ_2, thermal conductivity K_2, specific heat capacity C_{P2}. Body forces and body couples are neglected. The flow is set in by an applied pressure gradient in x-direction. The fluid velocities are taken as $\bar{q}_I = \left(u_I\left(y,t\right),0,0\right)$, where $I = 1,2$. This choice of velocities satisfies the equation of continuity. As the fluid velocity is unidirectional, the microrotation vector of region-I is assumed to be $\bar{\upsilon} = \left(0,0,c\left(y,t\right)\right)$. The fluid temperatures in both fluid regions are taken in the form $T_I = T_I(y,t)$, where $I = 1,2$.

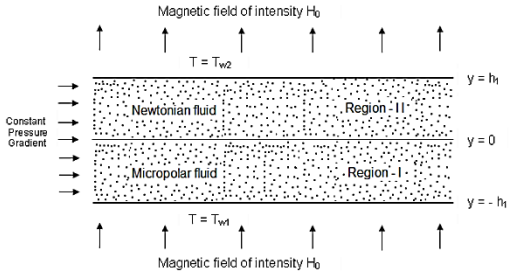

Fig. 1. Geometrical configuration of the problem.

Under the aforesaid circumstances, the equations governing the two-fluid flow are (Lukaszewicz (1999)).

Region-I: Micropolar fluid region ($-h_1 \le y \le 0$)

$$\rho_1\frac{\partial u_1}{\partial t} = \left(\mu_1 + \kappa\right)\frac{\partial^2 u_1}{\partial y^2} + \kappa\frac{\partial c}{\partial y} - \frac{\partial p}{\partial x} - \sigma {H_0}^2\bar{u}_1 - \frac{\mu_1}{k*}\bar{u}_1, \tag{1}$$

$$\rho_1 J\frac{\partial c}{\partial t} = \gamma\frac{\partial^2 c}{\partial y^2} - \kappa\left[\frac{\partial u_1}{\partial y} + 2c\right], \tag{2}$$

$$\rho_1 C_{P1}\frac{\partial T_1}{\partial t} = K_1\frac{\partial^2 T_1}{\partial y^2} + \mu_1\left(\frac{\partial u_1}{\partial y}\right)^2 + \kappa\left[\frac{\partial u_1}{\partial y} + 2c\right]^2 + \beta\left(\frac{\partial c}{\partial y}\right)^2, \tag{3}$$

Region-II: Newtonian fluid region ($0 < y \le h_1$)

$$\rho_2\frac{\partial u_2}{\partial t} = \mu_2\frac{\partial^2 u_2}{\partial y^2} - \frac{\partial p}{\partial x} - \sigma {H_0}^2\bar{u}_2 - \frac{\mu_2}{k*}\bar{u}_2, \tag{4}$$

$$\rho_2 C_{P2}\frac{\partial T_2}{\partial t} = K_2\frac{\partial^2 T_2}{\partial y^2} + \mu_2\left(\frac{\partial u_2}{\partial y}\right)^2. \tag{5}$$

It is to be mentioned here that, in the above, the last two terms of linear momentum Eqs. (1) and (4) are due to the appearance of magnetic field and the porous medium.

As the plates are stationary, in view of no-slip and hyperstick conditions at the boundary, velocities and microrotation are vanishing at the solid boundaries. By the virtue of coupling of fluid layers at the fluid-fluid interface through momentum transfer, we have continuous fluid velocities and continuous shear stresses at the interface.

Initially, fluids and plates are at fixed temperatures. The temperatures both the plates are taken as constant values T_{w1} and T_{w2} respectively, and the initial temperature of fluids is T_0*. Further, the temperature and heat flux are assumed to be continuous at interface of the fluids. Mathematically, the conditions are given as,

Initial Conditions:

$$u_1(y,0) = 0 \text{ for } -h_1 \le y \le 0, \tag{6}$$

$$u_2(y,0) = 0 \text{ for } 0 < y \le h_1, \tag{7}$$

$$c(y,0) = 0 \text{ for } -h_1 \le y \le 0, \tag{8}$$

$$T_1(y,0) = T_0* \text{ for } -h_1 \le y \le 0, \tag{9}$$

$$T_2(y,0) = T_0* \text{ for } 0 < y \le h_1, \tag{10}$$

Boundary and Interface Conditions: At $t > 0$,

$$u_1(-h_1,t) = 0 = u_2(h_1,t), \tag{11}$$

$$c(-h_1,t) = 0, \tag{12}$$

$$u_1(y,t) = u_2(y,t) \text{ at } y = 0, \tag{13}$$

$$\left(\mu_1 + \kappa\right)\frac{\partial u_1}{\partial y} + \kappa c = \mu_2\frac{\partial u_2}{\partial y} \text{ at } y=0, \tag{14}$$

$$c\left(y,t\right) = -\frac{1}{2}\frac{du_1}{dy} \text{ at } y=0, \tag{15}$$

$$T_1\left(-h_1,t\right) = T_{w_1}, \tag{16}$$

$$T_2\left(h_1,t\right) = T_{w_2}, \tag{17}$$

$$T_1(y,t) = T_2(y,t) \text{ at } y=0, \tag{18}$$

$$K_1 \frac{dT_1}{dy} = K_2 \frac{dT_2}{dy} \text{ at } y=0. \tag{19}$$

Using the non-dimensional parameters,

$$\bar{x} = \frac{x}{h_1}, \bar{y} = \frac{y}{h_1}, \bar{u}_1 = \frac{u_1}{U}, \bar{u}_2 = \frac{u_2}{U}, \bar{c} = \frac{h_1}{U}c, \bar{t} = \frac{U}{h_1}t,$$
$$\bar{p} = \frac{1}{U^2 \rho_1} p, \bar{T}_1 = \frac{T_1 - T_{w2}}{T_{w1} - T_{w2}}, \bar{T}_2 = \frac{T_2 - T_{w2}}{T_{w1} - T_{w2}}, \tag{20}$$

and assuming $\gamma = \left(\mu_1 + \frac{\kappa}{2}\right) J$, with $J = h_1^2$ (Ahmadi 1976), the governing Eqs. (1)-(5), after removing bars, come out to be,

Region-I: Micropolar fluid region ($-1 \le y \le 0$)

$$\frac{\partial u_1}{\partial t} = \frac{(1+n_1)}{Re}\frac{\partial^2 u_1}{\partial y^2} + \frac{n_1}{Re}\frac{\partial c}{\partial y} + G - \left[\frac{\left(M^2 + \frac{1}{Da}\right)}{Re}\right] u_1, \tag{21}$$

$$\frac{\partial c}{\partial t} = \frac{\left(1+\frac{n_1}{2}\right)}{Re}\frac{\partial^2 c}{\partial y^2} - \frac{n_1}{Re}\left[\frac{\partial u_1}{\partial y} + 2c\right], \tag{22}$$

$$\frac{\partial T_1}{\partial t} = \frac{1}{Re\,Pr}\frac{\partial^2 T_1}{\partial y^2} + \frac{Br}{Re\,Pr}\left[\left(\frac{\partial u_1}{\partial y}\right)^2 + n_1\left[\frac{\partial u_1}{\partial y} + 2c\right]^2 + \delta\left(\frac{\partial c}{\partial y}\right)^2\right], \tag{23}$$

Region-II: Newtonian fluid region ($0 < y \le 1$)

$$\frac{\partial u_2}{\partial t} = \frac{m_1}{Re\,m_2}\frac{\partial^2 u_2}{\partial y^2} + \frac{G}{m_2} - \left[\frac{M^2}{m_1} - \frac{1}{Da}\right] \times \frac{m_1}{Re\,m_2} u_2, \tag{24}$$

$$\frac{\partial T_2}{\partial t} = \frac{K}{Re\,Pr\,m_2\,C_P}\frac{\partial^2 T_2}{\partial y^2} + \frac{Br\,m_1}{Re\,Pr\,m_2\,C_P} \times \left(\frac{\partial u_2}{\partial y}\right)^2. \tag{25}$$

where $n_1 = \frac{\kappa}{\mu_1}, Re = \frac{\rho_1 U h_1}{\mu_1}, G = -\frac{\partial p}{\partial x}$,

$$M = \sqrt{\frac{\sigma H_0^2 h_1^2}{\mu_1}}, Da = \frac{k^*}{h_1^2}, Pr = \frac{\mu_1 C_{P1}}{K_1}, Br = \frac{\mu_1 U^2}{K_1 \Delta T},$$
$$\delta = \frac{\beta}{h^2 \mu_1}, m_1 = \frac{\mu_2}{\mu_1}, m_2 = \frac{\rho_2}{\rho_1}, K = \frac{K_2}{K_1}, C_P = \frac{C_{P2}}{C_{P1}},$$

Ignoring bars, the dimensionless conditions are

Initial conditions:

$$u_1(y,0) = 0 \text{ for } -1 \le y \le 0, \tag{26}$$

$$u_2(y,0) = 0 \text{ for } 0 < y \le 1, \tag{27}$$

$$c(y,0) = 0 \text{ for } -1 \le y \le 0, \tag{28}$$

$$T_1(y,0) = T_0 \text{ for } -1 \le y \le 0, \tag{29}$$

$$T_2(y,0) = T_0 \text{ for } 0 < y \le 1. \tag{30}$$

where $T_0 = \frac{T_0^* - T_{w2}}{T_{w1} - T_{w2}}$

Boundary and Interface conditions: At $t > 0$,

$$u_1(-1,t) = 0 = u_2(1,t), \tag{31}$$

$$c(-1,t) = 0, \tag{32}$$

$$u_1(0,t) = u_2(0,t), \tag{33}$$

$$(1+n_1)\frac{\partial u_1}{\partial y} + n_1 c = m_1 \frac{\partial u_2}{\partial y} \text{ at } y=0, \tag{34}$$

$$c(y,t) = -\frac{1}{2}\frac{du_1}{dy} \text{ at } y=0, \tag{35}$$

$$T_1(-1,t) = 1, \tag{36}$$

$$T_2(1,t) = 0, \tag{37}$$

$$T_1(y,t) = T_2(y,t) \text{ at } y = 0, \tag{38}$$

$$\frac{dT_1}{dy} = K\frac{dT_2}{dy} \text{ at } y=0. \tag{39}$$

3. NUMERICAL SOLUTION

The system of differential Eqs. (21)-(39) that governs the two-fluid flow situation is coupled and non-linear in nature, which makes the problem difficult for exact solution. Therefore, we implement an approach which finds numerical solution for the flow problem. One can identify that, the differential Eqs. (21), (22) and (24) are not coupled with the temperature; thus, once the flow characteristics i.e. velocities and microrotation are found from Eqs. (21),(22) and (24), the heat transfer characteristics can be obtained later on from Eqs. (23) and (25).

3.1 Velocity and Microrotation Distributions

A numerical approach based on Crank-Nicolson method is used to solve the PDEs (21),(22) and (24) subject to conditions (26)-(28) and (31)-(35). The domain [-1,1] is discretized uniformly with step sizes h and k in spatial and temporal directions respectively. Let (y_i,t_j) be a point in the considered domain, where i and j denote the spatial and temporal discretization parameters respectively. After discretization, the spatial domain for each time level is represented as $i = 0,1,2,3..F-1,F,F+1,F+2...l-1,l$, where $l\left(=\frac{2}{h}\right)$ is total number of mesh points in the discretized domain and $F\left(=\frac{l}{2}\right)$ is the interface

of two fluids. Note that, the boundary conditions (Eqs. (31)-(32)) are to be used at boundaries $i = 0$ and $i = l$, and, the interface conditions (Eqs. (33)-(35)) are to be used at interface $i = F$.

The finite difference approximations are used in the PDEs (21, 22, 24) and the Crank-Nicolson approach is followed. After simplifications, the finite difference schemes for distinct regions are found to be,

Region-I: Micropolar fluid region

($i = 1,2,3,.....F-1$)

$$\begin{aligned}&-A_4u_{1i-1,j+1}+A_1u_{1i,j+1}-A_4u_{1i+1,j+1}\\&+A_5c_{i-1,j+1}-A_5c_{i+1,j+1}\\&=A_3+A_4u_{1i-1,j}-A_2u_{1i,j}+A_4u_{1i+1,j}\\&-A_5c_{i-1,j}+A_5c_{i+1,j},\end{aligned}\tag{40}$$

$$\begin{aligned}&-A_6c_{i-1,j+1}+A_7c_{i,j+1}-A_6c_{i+1,j+1}\\&+A_5u_{1i+1,j+1}-A_5u_{1i-1,j+1}\\&=A_6c_{i-1,j}-A_8c_{i,j}+A_6c_{i+1,j}\\&-A_5u_{1i+1,j}+A_5u_{1i-1,j},\end{aligned}\tag{41}$$

Region-II: Newtonian fluid region

($i = F+1,F+2,.....l-1$)

$$\begin{aligned}&-A_9u_{2i-1,j+1}+A_{10}u_{2i,j+1}-A_9u_{2i+1,j+1}=\\&A_{11}+A_9u_{2i-1,j}-A_{12}u_{2i,j}+A_9u_{2i+1,j},\end{aligned}\tag{42}$$

where, $A_1=\left[1+\dfrac{k\left(1+n_1\right)}{h^2Re}+\dfrac{k\left(M^2+\dfrac{1}{Da}\right)}{2Re}\right], A_2=$

$\left[\dfrac{k\left(1+n_1\right)}{h^2Re}+\dfrac{k\left(M^2+\dfrac{1}{Da}\right)}{2Re}-1\right], A_3=kG, A_4=\dfrac{k\left(1+n_1\right)}{2h^2Re},$

$A_5=\dfrac{kn_1}{4hRe}, A_6=\dfrac{k\left(2+n_1\right)}{4h^2Re}, A_7=\left[1+\dfrac{k\left(2+n_1\right)}{2h^2Re}+\dfrac{kn_1}{Re}\right],$

$A_8=\left[\dfrac{k\left(2+n_1\right)}{2h^2Re}+\dfrac{kn_1}{Re}-1\right], A_9=\dfrac{km_1}{2m_2h^2Re},$

$A_{10}=\left[1+\dfrac{km_1}{m_2h^2Re}+\left(\dfrac{M^2}{m_1}+\dfrac{1}{Da}\right)\dfrac{km_1}{2Rem_2}\right], A_{11}=\dfrac{kG}{m_2},$

$A_{12}=\left[\dfrac{km_1}{m_2h^2Re}+\left(\dfrac{M^2}{m_1}+\dfrac{1}{Da}\right)\dfrac{km_1}{2Rem_2}-1\right].$

The conditions (26)-(28) and (31)-(35), in discretized form, take the form,

Initial conditions:

$u_{1i,j} = 0$, for $j = 0$ and $0 \le i \le F$, (43)

$u_{2i,j} = 0$, for $j = 0$ and $F < i \le l$, (44)

$c_{i,j} = 0$, for $j = 0$ and $0 \le i \le F$, (45)

Boundary and Interface conditions:

$u_{1i,j} = 0$ for $i = 0$ and for all j, (46)

$u_{2i,j} = 0$ for $i = l$ and for all j, (47)

$c_{i,j} = 0$ for $i = 0$ and for all j, (48)

$$\begin{aligned}&-Ru_{1F-1,j+1}+Su_{1F,j+1}-Tu_{2F+1,j+1}\\&+Lc_{F,j+1}=0,\end{aligned}\tag{49}$$

$$-Vu_{1F-1,j+1}+Vu_{1F,j+1}+c_{F,j+1}=0,\tag{50}$$

where,

$V=\dfrac{1}{2h}$, $R=\left(1+n_1\right), S=\left(1+n_1+m_1\right),$

$T=m_1$, $L=n_1h.$

The difference Eqs. (40), (41) and (42) contain unknowns of current time level in LHS and the known values of previous time level in RHS. After imposing the boundary conditions (46)-(48), out of total $(l+1)$ mesh points, we now are left with $(l-1)$ mesh points, where the numerical solution is aimed at.

For each time level j, for $i = 1,2,....,l-1$, the Eqs. (40)-(42) along with boundary and interface conditions Eqs. (46)-(50) compose a linear system of order $(l+F-1)$. In the matrix form, this system is written as,

$$ZX_{j+1}=YX_j+b,\ j=0,1,2,\ldots\tag{51}$$

where X_0 is given by initial conditions.

Here, Z and Y are matrices of banded sparse type. X_j is the solution of $(l+F-1)$ values at j^{th} time level and $b =$

$(A_3, A_3, ...A_3, 0, 0,...0, 0, A_{11}, A_{11},...A_{11})^{T}$ $_{(3F-1)\times1}$ is the known column vector in which middle $(F+1)$ entries are zero.

The linear system (51) is solved for each time level j to obtain the fluid fluid flow characteristics.

3.2 Rate of Volumetric Flow

The rate of volumetric flow is given in non-dimensional form as,

$$Q=\int_{-1}^{1}u(y,t)dy=\int_{-1}^{0}u_1(y,t)dy+\int_{0}^{1}u_2(y,t)dy.\tag{52}$$

Making use of the obtained numerical values of velocities $u_1(y,t)$ and $u_2(y,t)$, the volumetric flow rate across the channel is obtained by evaluating the integral (52) numerically.

3.3 Skin-Friction Coefficient

The expressions for skin friction coefficient at both plates are given by (2012),

at lower plate,

$$\left(C_f\right)_{y=-1}=\frac{2}{\mathrm{Re}}\left[\left(1+n_1\right)\frac{du_1}{dy}+n_1c\right]_{y=-1},$$

at upper plate.

$$\left(C_f\right)_{y=1} = \frac{2m_1}{\mathrm{Re}\, m_2}\left(\frac{du_2}{dy}\right)_{y=1},$$

Making use of the already obtained values of flow characteristics, the skin-friction co-efficient at both plates is computed from above expressions.

3.4 Temperature Distribution

This section aims at obtaining the numerical solution for temperature profiles for the considered two-fluid problem from Eqs. (23) and (25) using initial, boundary and interface conditions(29, 30, 36, 37, 38, 39).

The procedure in section (3.1) is followed for temperatures. The difference schemes for temperatures in respective flow regions, after simplification are given as

Region-I: Micropolar fluid region

(i = 1,2,3,.....$F-1$)

$$\begin{aligned}
&-C_1T_{1i-1,j+1} + \left(1+2C_1\right)T_{1i,j+1} - C_1T_{1i+1,j+1}\\
&= C_1T_{1i-1,j} + \left(1-2C_1\right)T_{1i,j} - C_1T_{1i+1,j}\\
&+C_2\Big[\left(u_{1i+1,j} - u_{1i-1,j}\right)^2\\
&+\left(u_{1i+1,j+1} - u_{1i-1,j+1}\right)^2\Big]\\
&+C_3\Bigg\{\left[\frac{u_{1i+1,j} - u_{1i-1,j}}{2h} + 2c_{i,j}\right]^2\\
&+\left[\frac{u_{1i+1,j+1} - u_{1i-1,j+1}}{2h} + 2c_{i,j+1}\right]^2\Bigg\}\\
&+C_4\Big[\left(c_{i+1,j} - c_{i-1,j}\right)^2\\
&+\left(c_{i+1,j+1} - c_{i-1,j+1}\right)^2\Big],
\end{aligned} \tag{53}$$

Region-II: Newtonian fluid region (i = F + 1,F + 2,.....$l-1$)

$$\begin{aligned}
&-C_5T_{2i-1,j+1} + \left(1+2C_5\right)T_{2i,j+1} - C_5T_{2i+1,j+1}\\
&= C_5T_{2i-1,j} + \left(1-2C_5\right)T_{2i,j} - C_5T_{2i+1,j}\\
&+C_6\Big[\left(u_{2i+1,j} - u_{2i-1,j}\right)^2\\
&+\left(u_{2i+1,j+1} - u_{2i-1,j+1}\right)^2\Big],
\end{aligned} \tag{54}$$

where $C_1 = \frac{k}{2h^2RePr}$, $C_2 = \frac{kBr}{8h^2RePr}$, $C_3 = \frac{kn_1Br}{2RePr}$, $C_4 = \frac{kBr\delta}{8h^2RePr}$, $C_5 = \frac{kK}{2h^2m_2RePrC_p}$, $C_6 = \frac{kBrm_1}{8h^2m_2RePrC_p}$

The conditions for temperature, in discretized version, are expressed as,

Initial conditions:

$$T_{1i,0} = T_0 \text{ for } 0 \le i \le F, \tag{55}$$

$$T_{2i,0} = T_0 \text{ for } F \le i \le l, \tag{56}$$

Boundary conditions:

$$T_{10,j} = 1 \text{ for all } j, \tag{57}$$

$$T_{2l,j} = 0 \text{ for all } j, \tag{58}$$

Interface condition: for all j,

$$-T_{1F-1,j+1} + \left(1+K\right)T_{1F,j+1} - KT_{2F+1,j+1} = 0. \tag{59}$$

Proceeding similarly as in case of section(3.1), after imposing initial, boundary and interface conditions, we arrive at the linear system,

$$\Theta\, T_{j+1} = \Upsilon + \Xi\, T_j, \text{ for all } j \tag{60}$$

where Θ and Ξ are matrices of tri-diagonal type of order $(l-1)$, and Υ is a known vector of $(l-1)$ quantities of fluid flow characteristics. For obtaining numerical values of fluid temperatures, the system (60) is solved at each time level.

3.5 Nusselt Number

The Nusselt number at lower and upper plate are respectively given by Ramana Murthy and Srinivas (2013),

$$\left(Nu\right)_{y=-1} = -\left(\frac{\partial T_1}{\partial y}\right)_{y=-1} \text{ and}$$

$$\left(Nu\right)_{y=1} = -\left(\frac{\partial T_2}{\partial y}\right)_{y=1}.$$

A finite difference approximation has been used to compute Nusselt number and its variation with pertinent flow parameters is presented through table 3.

4. RESULTS AND DISCUSSION

The model of time dependent two-fluid (Micropolar and Newtonian) flow is studied in presence of heat transfer effects through a porous channel. The magnetohydrodynamic effects are also considered while studying the problem. The system of differential equations that governs the aforesaid model is coupled and nonlinear. Hence, a numerical procedure based on Crank-Nicolson method is used to obtain the solution. The velocity and microrotation are obtained considering the spatial mesh-size to be 0.005, i.e. taking 401 × 401 grid, whereas, the temperature profiles are obtained considering 201 × 201 grid. The step size in time levels is taken to be 0.01. Figures 3-22 display the flow and heat transfer profiles for different sets of parameters arising in the considered fluid flow model. The study concerning volume flow rate, skin-friction and Nusselt number is displayed by means of tables (1), (2) and (3) respectively. Following is the set of fixed values of all parameters, while studying the flow and heat transfer. t = 0.5, n_1 = 0.5, Re = 1, Da = 0.2, M = 2, m1 = 0:5, Br = 0:4, K = 2, Pr = 0:4, Cp = 4, G = 5, d = 2. The obtained numerical results are validated by comparing them in the limiting case of non-MHD, non-porous and single Newtonian fluid (M = 0, Da = ∞, m_1 = 1, m_2 = 1,n_1 = 0) with the exact solutions of

Poiseuille flow of Newtonian fluid through a horizontal channel (Appendix). It is reported from Fig. 2 that a good agreement is seen between the limiting solution and the exact solution.

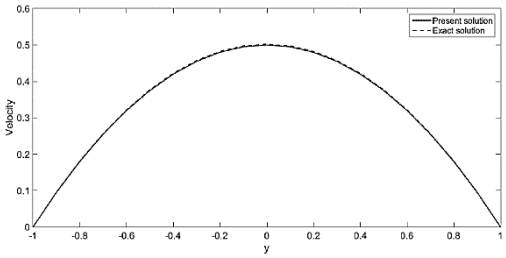

Fig. 2. Comparison of the present results with the exact solution

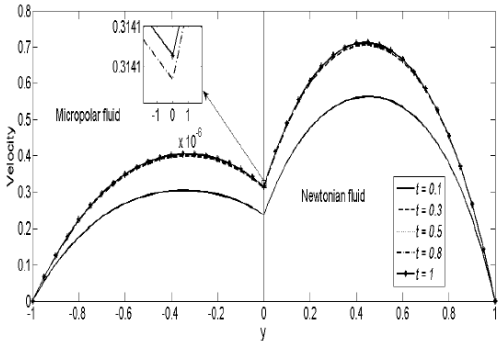

Fig. 3. Velocity profiles with varying time.

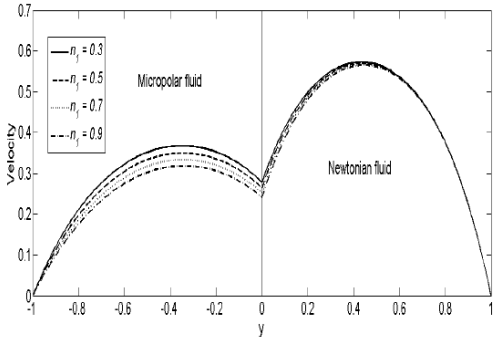

Fig. 4. Velocity profiles with varying micropolarity parameter.

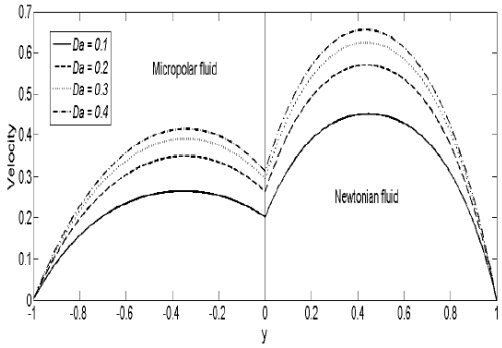

Fig. 5. Velocity profiles with varying Darcy number.

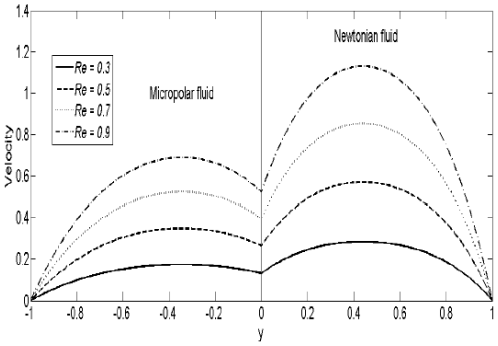

Fig. 6. Velocity profiles with varying Reynolds number.

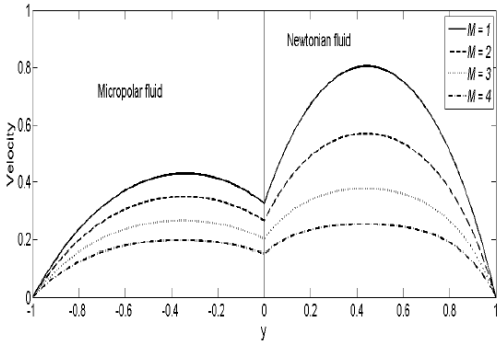

Fig. 7. Velocity profiles with varying Hartmann number.

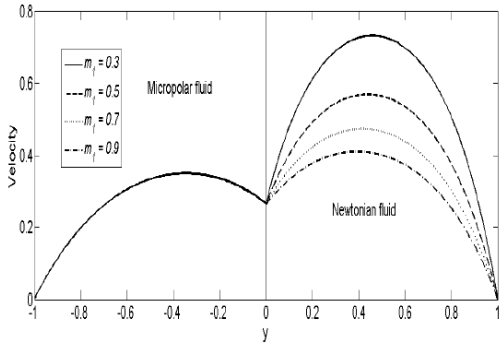

Fig. 8. Velocity profiles with varying viscosity ratio.

The impact of micropolarity parameter n_1, Reynolds number *Re*, Darcy number *Da*, Hartmann number *M* and ratio of viscosities m_1 on linear velocity is shown through Figs. 3-8. Figure 3 presents that, the fluid velocities are increasing with time and eventually for higher values of time, the flow is attaining steady state. The parameter n_1 is the micropolarity parameter, which represents measure of micropolarity effects in the fluid. It is noticed from Fig. 4 that, velocity in both regions is decreasing with increment of n_1. As $n_1\left(=\frac{\kappa}{\mu_1}\right)$ increases, the vortex viscosity κ increases which decreases the fluid velocity. Though n_1 is the feature of micropolar fluid alone, nevertheless, n_1 is affecting Newtonian fluid too in view of continuous fluid velocities and shear stresses. This is due to the coupling across the fluid-fluid interface. However, velocity decays slower in

Newtonian fluid region as compared to that of micropolar fluid region. The effect of uniform porous media is measured by a non-dimensional parameter called Darcy number $Da\left(=\frac{k^*}{h_1^2}\right)$, increasing of which leads to porous medium to clear medium. Figure 5 displays the increment in fluid velocities with the growing values of Darcy number *Da*. The reason being, the higher the Darcy number, the more the value of permeability parameter k^*, and evidently more permeable porous medium will provide a little restriction to the flow causing the fluid velocity to increase. As Darcy number goes higher and higher, the fluid medium becomes non-porous. The non-dimensional parameter $Re=\frac{\rho_1 U h_1}{\mu_1}$ is known as Reynolds number which is the ratio of inertial to viscous forces. Higher values of Reynolds number *Re* corresponds to lesser viscous forces in the fluid medium. As Reynolds number increases, there is a reduction in the viscous forces and hence increasing trend is seen in fluid velocities (see Fig. 6). The parameter $M=\sqrt{\frac{\sigma H_0^2 h_1^2}{\mu_1}}$ is known as Hartmann number and it measures the effects of applied transverse magnetic field. Figure 7 suggests that, increase of Hartmann number causes the velocity fields to decrease. This may be be due to the presence of applied transverse magnetic field acting on both plates, creating resistance to the fluid flow by means of the Lorentz force, which tend to pull the fluid velocities back. The increasing values of viscosity ratio cause a decline in velocities of fluids (see Fig. 8).

The behaviour of microrotation is shown through Figs. 9-14. Microrotation is also increasing with time and reaching steady state after a higher time level (see Fig. 9). It is depicted from Fig. 10 that, increase of micropolarity parameter n_1 causes a decrease in microrotation. It is evident from Figs. 11 and 13 that, increasing Darcy number leads to significant increase in microrotation, while increase in Hartmann number reduces the same. It is noted from Fig. 12 that, microrotation is increasing function of Reynolds number. Figure 14 presents that, incrementing of ratio of viscosities increases the microrotational velocity. However, the increase is much lower in magnitude.

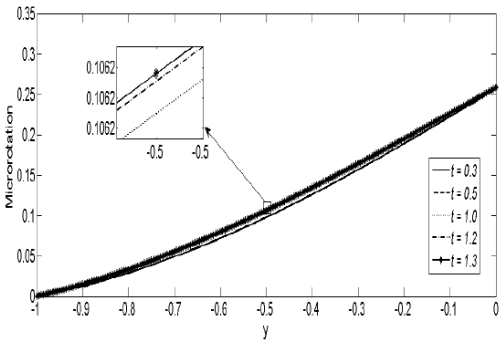

Fig. 9. Microrotation profiles with varying time.

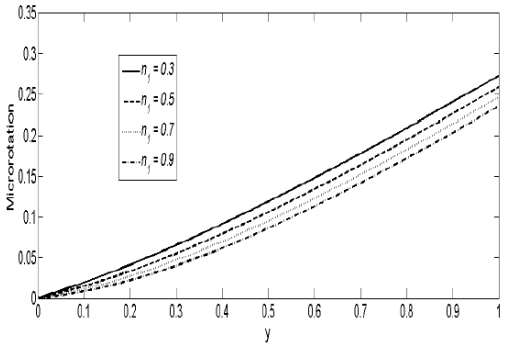

Fig. 10. Microrotation profiles with varying micropolarity parameter.

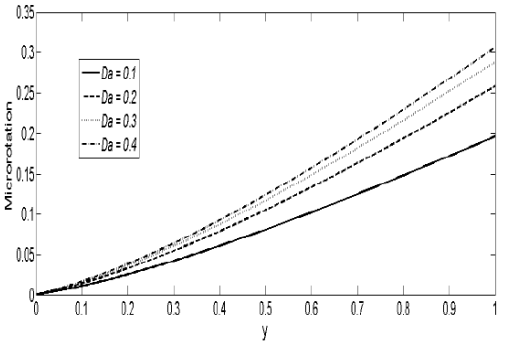

Fig. 11. Microrotation profiles with varying Darcy number.

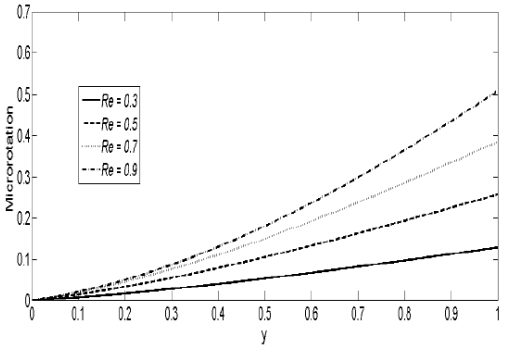

Fig. 12. Microrotation profiles with varying Reynolds number.

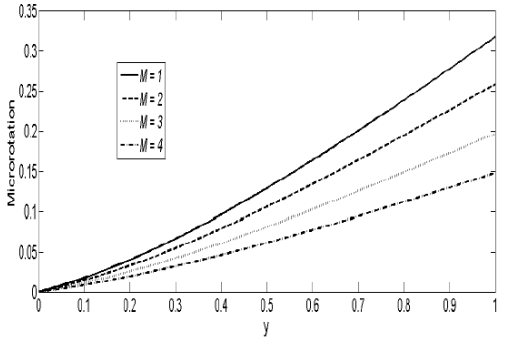

Fig. 13. Microrotation profiles with varying Hartmann number.

Figures 15-22 depict the effects of several parameters on heat transfer profiles. The viscous dissipation terms, which are nonlinear and dependent on the flow characteristics are not ignored during the

study. It is found from Fig. 15 that, temperature is growing with time in both fluid regions and is entering into a steady state. Figure 16 suggests that, the increasing micropolarity parameter n_1 is found to promote the temperature. However, the rate of this promotion is much leisure. Since the fluid velocities and microrotation are decreasing with increasing n_1, the energy dissipation from this flow fields decreases, and hence the temperature increases. Darcy number promotes the temperature fields (see Fig. 17). On the other hand, Hartmann number shows exactly opposite nature as that of Darcy number, i.e. temperature in both fluid regions got diminished by growing Hartmann number (see Fig. 19). Figure 18 depicts the effect of *Re* on heat transfer. In both flow regions, increase of Reynolds number causes the temperature profiles to increase.

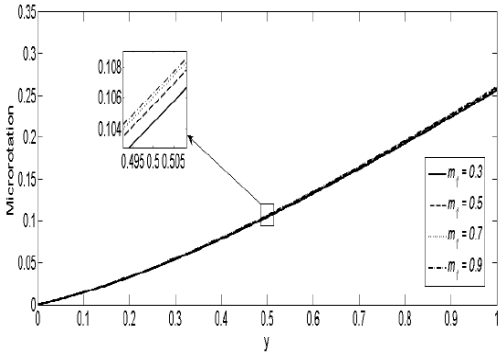

Fig. 14. Microrotation profiles with varying ratio of viscosities.

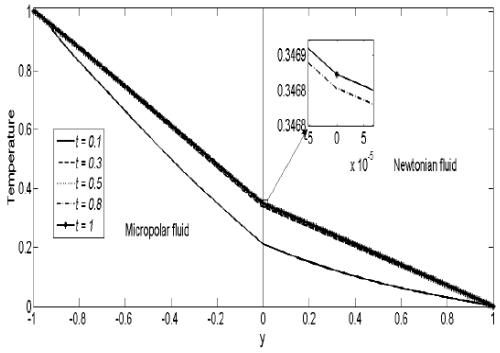

Fig. 15. Temperature profiles with varying time.

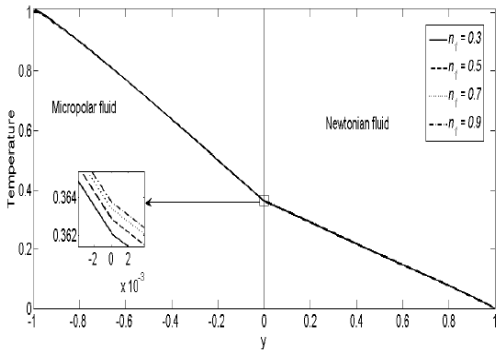

Fig. 16. Temperature profiles with varying micropolarity parameter.

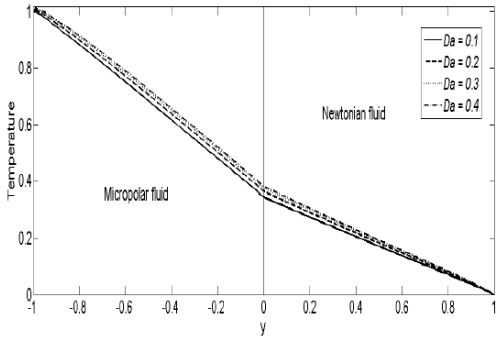

Fig. 17. Temperature profiles with varying Darcy number.

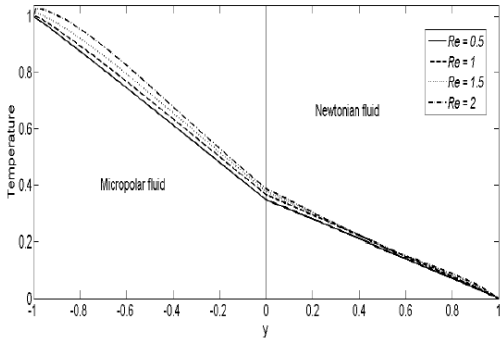

Fig. 18. Temperature profiles with varying Reynolds number.

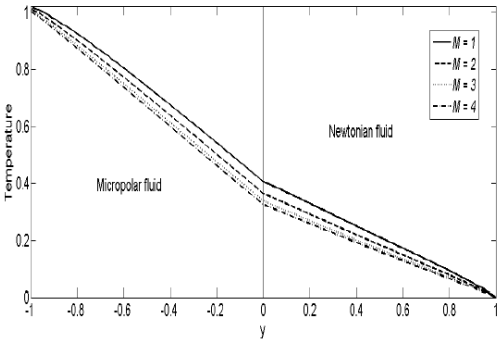

Fig. 19. Temperature profiles with varying Hartmann number.

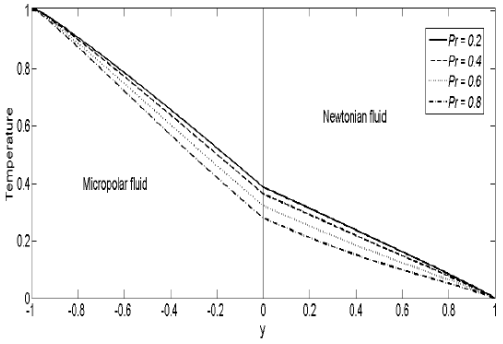

Fig. 20. Temperature profiles with varying Prandtl number.

Fluid temperatures are found to be increasing with Brinkmann number. Brinkman number *Br* is the ratio of heat produced by viscous dissipation and heat transported by molecular conduction. The

Table 1 Volume flow rate for various values of fluid parameters

n_1	Q		Re	Q		Da	Q
0.3	0.7261		0.5	0.3538		0.1	0.5558
0.5	0.7075		1	0.7075		0.2	0.7075
0.7	0.6909		1.5	1.0585		0.3	0.7792
0.9	0.6759		2	1.3982		0.4	0.8210

M	Q		M_1	Q		t	Q
1	0.9331		0.3	0.8335		0.3	0.7041
2	0.7075		0.5	0.7075		0.5	0.7075
3	0.5065		0.7	0.6343		1	0.7076
4	0.3638		0.9	0.5863		1.2	0.7076

greater its value of *Br*, the larger the rise in temperature. The same can be witnessed from Fig. 21. Figure 22 shows that, the thermal conductivity ratio is having a declining influence on temperature fields in both flow regions. Fluid temperatures with diverse values of Prandtl number can be noted from Fig. 20. The Prandtl number *Pr* is the non-dimensional number which quantifies the relative importance of viscosity and thermal conductivity. It is defined as the ratio of momentum to thermal diffusivity. Thus, as *Pr* increases, the viscous forces dominates over thermal forces resulting a decline in temperature. The same is evident from Fig. 20.

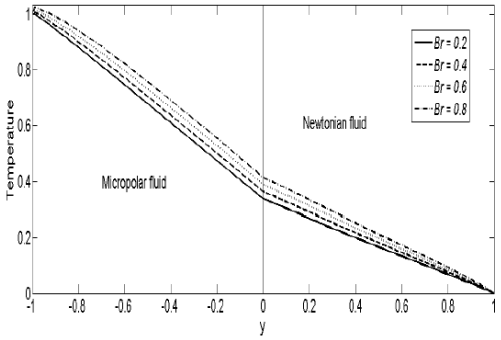

Fig. 21. Temperature profiles with varying Brinkmann number.

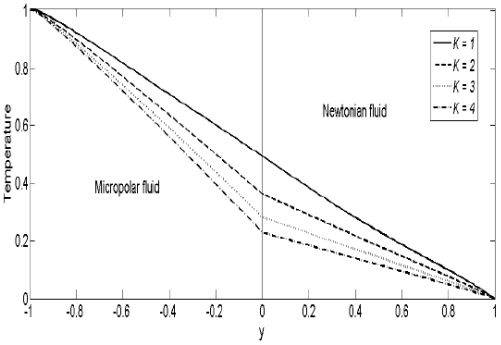

Fig. 22. Temperature profiles with varying ratio of thermal conductivities.

Table 1 unveil the numerical values for volume flow rate. It is observed that, volume flow rate falls down with the increasing n_1. As n_1 increases, velocity is decreasing, which lead to the noticed fall in the volume flow rate. A significant increase can be noted in volume flow rate with the increasing values of Reynolds number. The velocity fields are increasing with increasing values of Reynolds number, and hence there is a rise in volume flow rate. Hartmann number and Darcy number are having opposite impact on volume flow rate, which is quite obvious because increasing Hartmann number resists the flow and increasing Darcy number promotes the flow. Volume flow rate grows as time progresses and becomes constant after certain time value which confirms the fact that the fluid flow reaches steady state after certain time level**.**

As the fluid flows over plates, it applies frictional force on the surface of the plates which works to impede forward movement of the plates, hence imparting skin friction drag on the object. This drag is measured by skin-friction co-efficient. Table 2 depicts that, at lower plate of the channel, skin friction increases with micropolarity parameter and Darcy number whereas it decreases with the increasing values of Reynolds number, Hartmann number and viscosity ratio. At upper plate, increasing values of n_1, *Re*, *M* and m_1 are responsible for the increase of skin friction co-efficient. Darcy number reduces the same at upper plate. Skin friction co-efficient when varied with time, at lower plate, it got enhanced, and at upper plate, got reduced, and become constant eventually at both the plates.

Table 3 displays the behaviour of Nusselt number at the channel plates. At lower plate, Nusselt number is enhanced by the enhancement of micropolarity parameter, Hartmann number, ratio of viscosities and time, while Nusselt number is reduced with Reynolds number, Brinkmann number, Darcy number, Prandtl number and ratio of specific heats. On the other hand, at upper plate, Nusselt number grows with the increase of micropolarity parameter, Reynolds number, Brinkmann number and Darcy number. Further, Hartmann number, ratio of viscosities and time are having reducing impact on Nusselt number at upper plate.

5. CONCLUSIONS

The unsteady MHD flow and heat transfer of immiscible micropolar and Newtonian fluids

Table 2 Skin friction co-efficient for various values of fluid parameters

n_1	$(c_f)_{y=-1}$	$(c_f)_{y=1}$	Re	$(c_f)_{y=-1}$	$(c_f)_{y=1}$
0.3	3.3694	-4.8868	0.5	3.6008	-4.8819
0.5	3.5999	-4.8817	1	3.5999	-4.8817
0.7	3.8043	-4.8769	1.5	3.5875	-4.8764
0.9	3.9872	-4.8726	2	3.5510	-4.8566

Da	$(c_f)_{y=-1}$	$(c_f)_{y=1}$	M	$(c_f)_{y=-1}$	$(c_f)_{y=1}$
0.1	2.9553	-4.1564	1	4.2031	-6.3228
0.2	3.5999	-4.8817	2	3.5999	-4.8817
0.3	3.9065	-5.2057	3	2.9554	-3.6641
0.4	4.0859	-5.3899	4	2.4159	-2.8192

m_1	$(c_f)_{y=-1}$	$(c_f)_{y=1}$	t	$(c_f)_{y=-1}$	$(c_f)_{y=1}$
0.3	3.6090	-4.1085	0.3	3.5783	-4.8718
0.5	3.5999	-4.8817	0.5	3.5999	-4.8817
0.7	3.5952	-5.3696	1	3.6009	-4.8819
0.9	3.5923	-5.7221	1.2	3.6009	-4.8819

Table 3 Nusselt number for various values of fluid parameters

n_1	$(Nu)_{y=-1}$	$(Nu)_{y=1}$		Re	$(Nu)_{y=-1}$	$(Nu)_{y=1}$		Br	$(Nu)_{y=-1}$	$(Nu)_{y=1}$
0.3	0.1891	0.4578		0.5	0.5549	0.3650		0.2	0.4281	0.4033
0.5	0.2042	0.4584		1	0.2042	0.4584		0.4	0.2042	0.4584
0.7	0.2199	0.4588		1.5	-0.3526	0.5992		0.6	-0.0197	0.5135
0.9	0.2356	0.4590		2	-1.0544	0.7582		0.8	-0.2436	0.5687

Da	$(Nu)_{y=-1}$	$(Nu)_{y=1}$		M	$(Nu)_{y=-1}$	$(Nu)_{y=1}$		Pr	$(Nu)_{y=-1}$	$(Nu)_{y=1}$
0.1	0.3900	0.4188		1	-0.0370	0.5571		0.2	0.2151	0.4516
0.2	0.2042	0.4584		2	0.2042	0.4584		0.4	0.2042	0.4584
0.3	0.0961	0.4795		3	0.3954	0.4004		0.6	0.1854	0.4778
0.4	0.0269	0.4925		4	0.5085	0.3737		0.8	0.1675	0.5006

m_1	$(Nu)_{y=-1}$	$(Nu)_{y=1}$		t	$(Nu)_{y=-1}$	$(Nu)_{y=1}$		C_P	$(Nu)_{y=-1}$	$(Nu)_{y=1}$
0.3	0.1778	0.4671		0.3	0.188	0.4856		2	0.2137	0.4511
0.5	0.2042	0.4584		0.5	0.2042	0.4585		4	0.2042	0.4584
0.7	0.2197	0.4481		1	0.2129	0.4496		6	0.1868	0.4814
0.9	0.2299	0.4395		1.2	0.2131	0.4493		8	0.1669	0.5122

through a channel filed with porous medium has been investigated. The Crank-Nicolson finite difference technique has been employed to acquire the numerical solution.

The main outcomes of the current work are presented hereunder:

- The obtained numerical results are found to be in good agreement, in the limiting case, with the exact solution of Newtonian fluid flow.
- After increasing with time initially, the fluid velocities, microrotation and fluid temperatures are increasing with time and attaining steady state at certain higher time level.
- The presence of micropolarity effects are reducing fluid velocities.
- The fluid temperatures are promoted by increasing micropolarity parameter.
- The Brinkmann number is increasing the temperature profiles while the Prandtl number is lessening it**.**

ACKNOWLEDGEMENTS

The authors are indebted to National Board for Higher Mathematics, Department of Atomic Energy, India, for the financial aid Ref. No.2/48(23)/2014/NBHM-R&D II/1083 dated 28-01-2015. Authors also thank the reviewers for their suggestions, which helped in strengthening the work.

REFERENCES

Abdullaha, I. and N. Amin (2010). A micropolar fluid model of blood flow through a tapered artery with a stenosis. *Mathematical Methods in the Applied Sciences* 33, 1910-1923.

Ahmadi, G. (1976). Self similar solution of incompressible micropolar boundary layer flow over a semi-infinite plate. *International Journal of Engineering Science* 14, 639-646.

Allen, S. J. and K. A. Kline (1971). Lubrication theory for micropolar fluids. *Journal of Applied Mechanics* 38(3), 646-650.

Ariman, T., M. A. Turk and N. D. Sylvester (1973). Microcontinum fluid mechanicsa review. *International Journal of Engineering Science* 11, 905-930.

Ariman, T., M. A. Turk and N. D. Sylvester (1974). Application of microcontinum fluid mechanics. *International Journal of Engineering Science* 12, 273-293.

Ashraf, M., N. Jameel and K. Ali (2013). MHD non-Newtonian micropolar fluid flow and heat transfer in channel with stretching walls. *Applied Mathematics and Mechanics* 34(10), 1263-1276.

Bataineh, A. S., M. S. M. Noorani and I. Hashim (2009). Solution of fully developed free convection of a micropolar fluid in a vertical channel by homotopy analysis method. *International Journal for Numerical Methods in Fluids* 60, 779-789.

Bhargava, R., L. Kumar and H. S. Takhar (2003). Numerical solution of free convection MHD micropolar fluid flow between two parallel porous vertical plates. *International Journal of Engineering Science* 41, 123-136.

Bird, R. B., W. E. Stewart and E. N. Lightfoot (1960). *Transport Phenomena*. New York: John Wiley and Sons.

Chamkha, A. J. (2000). Flow of two immiscible fluids in porous and nonporous channel. *Journal of Fluids Engineering* 121, 117-124.

Chaturani, P. and R. P. Samy (1985). A study of non-Newtonian aspects of blood flow through stenosed arteries and its applications in arterial diseases. *Biorheology* 22, 521-531.

Cheng, C. Y. (2006). Fully developed natural convection heat and mass transfer of a micropolar fluid in a vertical channel with asymmetric wall temperatures and concentrations. *International Communications in Heat and Mass Transfer* 33, 627-635 .

Crank, J. and P. Nicolson (1947). A practical method for numerical evaluation of solutions of partial differential equations of the heat conduction type. *Mathematical Proceedings of the Cambridge Philosophical Society* 43(1), 50-67.

Eringen, A. C. (1966). Theory of micropolar fluids. *International Journal of Mathematics and Mechanics* 16, 1-18.

Eringen, A. C. (2000). *Microcontinuum Field Theories II: Fluent Media*. New York: Springer.

Kang, C. K. and A. C. Eringen (1976). The effect of microstructure on the rheological properties of blood. *Bulletin of Mathematical Biology* 38, 135-159.

Kapur, J. N. and J. B. Shukla (1962). The flow of incompressible immiscible fluids between two parallel plates. *Applied Sciences* 13, 55-60.

Kumar, N. and S. Gupta (2012). MHD freeconvective flow of micropolar and Newtonian fluids through porous medium in a vertical channel. *Meccanica* 47, 277-291.

Lukaszewicz, G. (1999). *Micropolar Fluids, Theory and Applications*. Birkhauser, Boston: Springer.

Mabood, F. and S. M. Ibrahim (2016). Effects of soret and non-uniform heat source on MHD non-Darcian convective flow over a stretching sheet in a dissipative micropolar fluid with radiation. *Journal of Applied Fluid Mechanics* 9(5), 2503-2513.

Mekheimer, Kh. S. and M. A. El. Kot (2008). The micropolar fluid model for blood flow through a tapered artery with a stenosis. *Acta Mechanica Sinica* 24, 637-644.

Naduvinamani, N. B. and S. Santosh (2011). Micropolar fluid squeeze film lubrication of finite porous journal bearing. *Tribology International* 44(4), 409-416.

Nikodijevic, D., D. Milenkovic and Z. Stamenkovic (2011). MHD Couette two-fluid flow and heat transfer in presence of uniform inclined magnetic field. *Heat and Mass Transer* 47, 1525-1535.

Prasad, K. V., K. Vajravelu, P. S. Datti and B. T. Raju (2013). MHD Flow and Heat Trans-fer in a Power-law Liquid Film at a Porous Surface in the Presence of Thermal Radiation. *Journal of Applied Fluid Mechanics* 6(3), 385-395.

Prathap Kumar, J., J. C. Umavathi, A. J. Chamkha and I. Pop (2010). Fully-developed free-convective flow of micropolar and viscous fluids in a vertical channel. *Applied Mathematical Modelling* 34, 1175-1186.

Ramana Murthy, J. V. and J. Srinivas (2013). Second law analysis for Poiseuille flow of immiscible micropolar fluids in a channel. *International Journal of Heat and Mass Transfer* 65, 254-264.

Ramesh, K. and M. Devakar (2015a). Magnetohydrodynamic peristaltic transport of couple stress fluid through porous medium in an inclined asymmetric channel with heat transfer. *Journal of Magnetism and Magnetic Materials* 394, 335-348.

Ramesh, K. and M. Devakar (2015b). The Influence of Heat Transfer on Peristaltic Transport of MHD Second Grade Fluid through Porous Medium in a Vertical Asymmetric Channel. *Journal of Applied Fluid Mechanics* 8(3), 351-365.

Sai, K. S. (1990). Unsteady Flow of Two Immiscible Viscous Fluids Over a Naturally Permeable

Bed. *Defence Science Journal* 40, 183-189.

Singh, A. K. (2005). Convective flow of two immiscible viscous fluids using Brinkmann model. *Indian Journal of Pure and Applied Physics* 43, 415-421.

Stokes, V. K. (1971). Effects of couple stresses in fluids on the creeping flow past a sphere. *Physics of fluids* 14(7), 1580-1582.

Stokes, V. K. (1984). *Theories of fluids with microstructure - an introduction.* New-York: Springer-Verlag.

Tetbirt, A., M. N. Bouaziz and M. Tahar Abbes (2016). Numerical study of magnetic effect on the velocity distribution field in a macro/micro-scale of a micropolar and viscous fluid in vertical channel. *Journal of Molecular Liquids* 216, 103-110.

Umavathi, J. C., A. J. Chamkha, A. Mateen and A. AlMudhaf (2005). Unsteady two-fluid flow and heat transfer in a horizontal channel. *Heat and Mass Transfer* 42, 81-90.

Umavathi, J. C., I. C. Liu and M. Shekar (2012). Unsteady mixed convective heat transfer of two immiscible fluids confined between long vertical wavy wall and parallel flat wall. *Applied Mathematics and Mechanics* 33, 931-950.

Vajravelu, K., P. V. Arunachalam and S. Sreenadh (1995). Unsteady flow of two immiscible conducting fluids between two permeable beds. *Journal of Mathematical Analysis and Applications* 196. 1105-1116.

Zivojin, S. M., D. D. Nikodijevic, B. D. Blagojevic and S. R. Savic (2010). MHD flow and heat transfer of two immiscible fluids between moving plates. *Transactions of the Canadian Society for Mechanical Engineering* 34, 3-4.

APPENDIX

The governing equations for the steady flow of single Newtonian fluid through the horizontal channel (Fig. 1) are simplified as

$$-\frac{dp}{dx}+\mu\frac{d^2u}{dy^2}=0 \tag{61}$$

with the boundary conditions,

$$u\left(\pm h_1\right)=0. \tag{62}$$

Using the non-dimensional scheme (20), the Eqs. (61) and (62) become

$$\frac{d^2u}{dy^2}+ReG=0 \tag{63}$$

$$\text{with } u\left(\pm 1\right)=0. \tag{64}$$

The exact solution of the boundary value problem Eqs. (63)-(64) is obtained as

$$u\left(y\right)=\frac{ReG}{2}\left[1-y^2\right]. \tag{65}$$